J|A|C|S
ARTICLES
Published on Web 08/10/2002

Regioselective Silylation of Sugars through Palladium Nanoparticle-Catalyzed Silane Alcoholysis

Mee-Kyung Chung,[§] Galina Orlova,[§] John D. Goddard,[§] Marcel Schlaf,*[,§] Robert Harris,[†] Terrance J. Beveridge,[†] Gisele White,[‡] and F. Ross Hallett[‡]

Contribution from the Guelph-Waterloo Centre for Graduate Work in Chemistry (GWC²), Department of Chemistry and Biochemistry, NSERC Guelph Regional STEM Facility, Department of Microbiology, and Guelph Biophysics Light Scattering Laboratory, Department of Physics, University of Guelph, Guelph, Ontario, Canada, N1G 2W1

Received April 29, 2002

Abstract: Palladium(0)-catalyzed silane alcoholysis was applied to sugars for the first time using *tert*-butyldimethylsilane (TBDMS-H) and Ph_3SiH as the silanes. The catalyst is a colloidal solution of Pd(0) generated in situ from PdX_2 ($X = Cl^-$, OAc^-) and TBDMS-H in *N,N*-dimethylacetamide. The colloid has been characterized by dynamic light scattering and transmission electron microscopy and consists of catalytically highly active nanoparticles of ~2 nm diameter. The silane alcoholysis reaction is an effective method for the regioselective silylation of methyl and phenyl glycosides and generates hydrogen gas as the only side product. For many of the sugar substrates investigated, the distribution of regioisomers obtained is complementary to that of the traditional R_3SiCl/base (base = pyridine, imidazole) methodology and gives convenient access to the 3,6- rather than the 2,6-silylated pyranosides, obtained as the main product by the silyl chloride method. The method also allows a selective axial silylation of levoglucosan and 1,3,5-*O*-methylidene-*myo*-inositol. In an attempt to rationalize the observed regioselectivities, ab initio predictions (HF/3-21G*) have been made on the relative energies of some of the silylated products. They suggest that the observed regioselectivities do not reflect a kinetic vs thermodynamic product distribution but are induced by the silylation agent employed. Models for the possible origin of the observed regioselectivity in both silylation methods (silane- and silyl chloride-based) are discussed.

Introduction

Silyl ethers are versatile protecting groups for hydroxyl functions and are routinely used in carbohydrate chemistry.[1] The standard method for the silylation of a sugar hydroxyl function is the reaction of the sugar substrate with a trialkylsilyl chloride or mixed alkyl/arylsilyl chloride in the presence of excess base, typically either imidazole in *N,N*-dimethylformamide (DMF) solvent or pyridine, which acts as both the solvent and base at the same time (eq 1).

$$R{-}OH + R'R''R'''SiCl + B \rightarrow R{-}O{-}SiR'R''R''' + HB^+Cl^- \quad (1)$$

R = sugar; R′,R″,R‴ = alkyl or aryl; B = pyridine, imidazole

The use of trimethylsilyl chloride with this method allows the rapid persilylation of sugars and polyols, rendering them volatile enough for GC analysis.[2,3] For synthetic purposes, *tert*-butyldimethylsilyl chloride (TBDMS-Cl) and *tert*-butyldiphenylsilyl chloride (TBDPS-Cl) have emerged as the silylation reagents of choice, as the resulting silyl ethers strike the right balance between stability under acidic or basic conditions and ease of selective removal, e.g., by reaction with tetrabutylammonium fluoride[4−7] or catalytic amounts of CBr_4 in methanol.[8] With TBDMS-Cl, a regioselective silylation of otherwise unprotected methyl pyranosides of glucose, mannose, and galactose has been achieved. Six-position monosilylated as well as 2,6-disilylated and in some cases 2,4,6- and 2,3,6-trisilylated pyranosides are accessible by this method in moderate to good yields.[9−11] When the reaction is mediated by equimolar amounts of dibutyltin oxide, the silylation of methyl α-D-pyranosides of glucose, mannose, and galactose with TBDMS-Cl gives the 6-monosilylated products in excellent yields.[12]

* Address correspondence to this author. E-mail: mschlaf@uoguelph.ca.
[§] Guelph-Waterloo Centre for Graduate Work in Chemistry, Department of Chemistry and Biochemistry.
[†] NSERC Guelph Regional STEM Facility, Department of Microbiology.
[‡] Guelph Biophysics Light Scattering Laboratory, Department of Physics.

(1) Collins, P.; Ferrier, R. *Monosaccharides*; John Wiley & Sons: Toronto, 1995.
(2) Dutton, G. S. *Adv. Carbohydr. Chem. Biochem.* **1973**, *28*, 12−160.
(3) Andrews, M. A. *Carbohydr. Res.* **1989**, *194*, 1−19.
(4) Corey, E. J.; Venkateswarlu, A. *J. Am. Chem. Soc.* **1972**, *94*, 6190−6191.
(5) Hanessian, S.; Lavallee, P. *Can. J. Chem.* **1975**, *53*, 2975−2977.
(6) Mulzer, J.; Schöllhorn, B. *Angew. Chem., Int. Ed. Engl.* **1990**, *29*, 431−432.
(7) Kraska, B.; Klemer, A.; Hagedorn, H. *Carbohydr. Res.* **1974**, *36*, 398−403.
(8) Chen, M.-Y.; Lu, K.-C.; Lee, A. S.-Y.; Lin, C.-C. *Tetrahedron Lett.* **2002**, *43*, 2777−2780.
(9) Franke, F.; Guthrie, R. D. *Aust. J. Chem.* **1977**, *30*, 639−647.
(10) Brandstetter, H. H.; Zbiral, E. *Helv. Chim. Acta* **1978**, *61*, 1832−1841.
(11) Halmos, T.; Montserrat, R.; Filippi, J.; Anonakis, K. *Carbohydr. Res.* **1987**, *170*, 57−69.
(12) Bredenkamp, M. W. *S. Afr. J. Chem.* **1995**, *48*, 154−156.

10.1021/ja026723v CCC: $22.00

The transition metal-catalyzed silane alcoholysis reaction shown in eq 2 presents an attractive alternative method for the synthesis of silyl ethers that does not generate stoichiometric amounts of pyridinium or imidazolium chloride but gives hydrogen gas as the only side product, resulting in very simple reaction protocols and workup procedures.

$$\mathrm{R{-}OH + R'R''R'''SiH \xrightarrow{[cat.]} R{-}O{-}SiR'R''R''' + H_2(g)}$$
$$\mathrm{R = sugar;\ R',R'',R''' = alkyl\ or\ aryl} \qquad (2)$$

The silane alcoholysis reaction is efficiently catalyzed by a wide variety of transition metal complexes,[13−26] the Lewis acid $B(C_6F_5)_3$,[27] and most simply palladium, nickel, and ruthenium metal.[28] For a comprehensive review on the reaction, see Lukevics and Dzintara.[29]

Building on the earlier work by Sommer and Lyons,[28] who first demonstrated the use of Pd(0) as a silane alcoholysis catalyst, we have now found that a palladium nanoparticle colloid generated in situ in *N*,*N*-dimethylacetamide (DMA) solvent from PdX_2 (X = Cl^-, OAc^-) and *tert*-butyldimethylsilane (TBDMS-H) or triphenyl silane is an effective catalyst for the regioselective silylation of sugars. For the first time, we have applied this reaction to a series of methyl pyranosides of glucose, mannose, galactose, xylose, and arabinose as well as the derivatives 1,5-anhydro-xylitol, arabinitol, 1,6-anhydro-*β*-glucopyranoside, and 1,3,5-*O*-*myo*-inositol and investigated the regioselectivity and mechanism of the palladium-catalyzed silane alcoholysis reaction in direct comparison to the *classical* silyl chloride method.

Choice of Sugar Substrate. Because of their high natural abundance and biological significance, we focused our study on glucose, mannose, and galactose and some of their corresponding pentoses and 1-deoxy-cyclitols. Due to mutarotation, the reaction of free sugars with TBDMS-H/Pd(0) or TBDMS-Cl/base gives intractable complex reaction mixtures and is consequently not of synthetic value. Therefore, the methyl and in one case phenyl glycosides as the simplest glycosides of the sugars were employed as the first series of substrates. Also investigated were 1,6-anhydro-*β*-glucopyranoside and 1,3,5-*O*-methylidene-*myo*-inositol. For reference throughout this paper, the structures of all sugar substrates investigated with their numbering scheme are shown in Chart 1.

Choice of Solvent, Catalyst, and Silane. To date, catalytic silane alcoholysis reactions have been carried out only in nonpolar solvents such as methylene chloride, toluene, and pentane, which are incompatible with the highly polar and lipophobic sugar substrates. In a recent study that employed ethylene glycol and Et_3SiH as a model system, we therefore evaluated several silane alcoholysis catalysts in the highly polar yet unreactive solvent DMA, which dissolves sugars and at the same time is compatible with various transition metal-based catalysts.[30] From this study, Pd(0) generated in situ from either $PdCl_2$ or $Pd(OAc)_2$ and the silane emerged as one of the most active and—since no catalyst synthesis is involved—most easily handled catalyst systems and was therefore selected for the present study. The choice of TBDMS-H as the silane is based on the properties of the well-established TBDMS-Cl-derived silyl ethers discussed above and its low tendency for migration when several hydroxyl functions are present.[4,9−11]

Chart 1

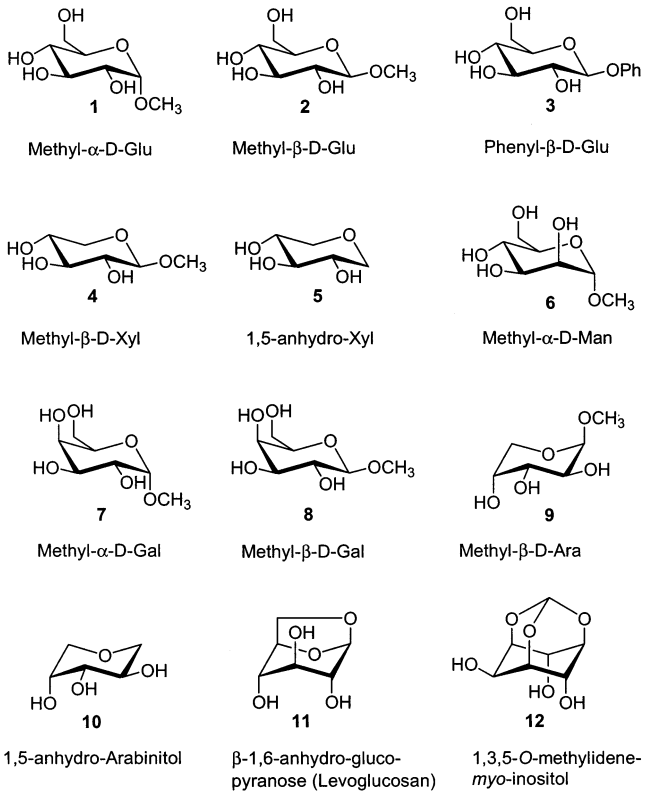

Numbering scheme:
 # a: Monosilylated in position 6 with TBDMS
 # b: 2,6-disilylated with TBDMS (2-monosilylated for Xyl, Ara and Ino)
 # c: 3,6-disilylated with TBDMS (3-monosilylated for Xyl and Ara)
 # d: 4,6-disilylated with TBDMS (4-monosilylated for Xyl, Ara and Ino)
 # e: 2,4-disilylated with Ph_3Si for Lev and Ino
 # f: 2,4-disilylated with TBDMS for Ino

Results

Silylation Reactions. All silane alcoholysis reactions were carried out by first generating a black solution of the active Pd(0) catalyst colloid by reacting PdX_2 (3 mol %, X = Cl^-, OAc^-) with 0.3−3.3 equiv (with respect to sugar) of TBDMS-H in DMA and then adding a second solution of the sugar in DMA. The reaction progress was monitored by analytical TLC, and completion of the reaction was indicated by the cessation of hydrogen gas evolution and precipitation of bulk palladium

(13) Doyle, M. P.; Higgins, K. G.; Bagheri, V.; Pieters, R. J.; Lewis, P. J.; Pearson, M. M. *J. Org. Chem.* **1990**, *55*, 6082−6086.
(14) Barton, D. H.; Kelly, M. J. *Tetrahedron Lett.* **1992**, *33*, 5041−5044.
(15) Bedard, T. C.; Corey, J. Y. *J. Organomet. Chem.* **1992**, *428*, 315−333.
(16) Gregg, B. T.; Cutler, A. R. *Organometallics* **1994**, *13*, 1039−1043.
(17) Burn, M. J.; Bergman, R. G. *J. Organomet. Chem.* **1994**, *472*, 43−54.
(18) Lorenz, C.; Schubert, U. *Chem. Ber.* **1995**, *128*, 1267−1269.
(19) Chang, S.; Scharrer, E.; Brookhart, M. *J. Mol. Catal. A* **1998**, *130*, 107−119.
(20) Luo, X.-L.; Crabtree, R. H. *J. Am. Chem. Soc.* **1989**, *111*, 2527−2535.
(21) Oehmichen, U.; Singer, H. *J. Organomet. Chem.* **1983**, *243*, 199−204.
(22) Chalk, A. J. *J. Chem. Soc., Chem. Commun.* **1970**, 847−848.
(23) Ojima, I.; Kogure, T.; Nihonyanagi, M.; Kono, H.; Inaba, S. *Chem. Lett.* **1973**, 501−504.
(24) Corriu, R. J. P.; Moreau, J. J. E. *J. Organomet. Chem.* **1976**, *114*, 135−144.
(25) Corriu, R. J.; Moreau, J. J. E. *J. Chem. Soc., Chem. Commun.* **1973**, 38−39.
(26) Blackburn, S. N.; Haszeldien, R. N.; Parish, R. V. *J. Organomet. Chem.* **1980**, *192*, 329−338.
(27) Blackwell, J. M.; Foster, K. L.; Beck, V. H.; Piers, W. E. *J. Org. Chem.* **1999**, *64*, 4887−4892.
(28) Sommer, L. H.; Lyons, J. E. *J. Am. Chem. Soc.* **1969**, *91*, 7061−7066.
(29) Lukevics, E.; Dzintara, M. *J. Organomet. Chem.* **1985**, *295*, 265−315.
(30) Chung, M.-K.; Ferguson, G.; Robertson, V.; Schlaf, M. *Can. J. Chem.* **2001**, *79*, 949−957.

Table 1. Isolated Yields for the Selective Monosilylation of 6-OH of Methyl Hexopyranosides with PdX_2 (X = Cl^-, OAc-) 3 mol %)/ ^{t}BuMe$_2$SiH and ^{t}BuMe$_2$SiCl/Base

entry	sugar substrate	catalyst precursor	temp (°C)	amount of TBDMS-H (equiv)	yield with TBDMS-H/PdX_2 (%)	yield with TBDMS-Cl/base (%)
1	methyl α-D-Glu (**1**)	$Pd(OAc)_2$	25	3.5	94	95;[a] 76;[b] 90[c]
2	methyl β-D-Glu (**2**)	$PdCl_2$	25	1.3	71	74[d]
3	phenyl β-D-Glu (**3**)	$Pd(OAc)_2$	35	1.2	78	81[e]
4	methyl α-D-Man (**6**)	$Pd(OAc)_2$	25	1.3	73	84;[c] 77[f]
5	methyl α-D-Gal (**7**)	$PdCl_2$	25	1.6	62	92[c]
6	methyl β-D-Gal (**8**)	$Pd(OAc)_2$	35	1.3	67	72;[g] 77[f]

[a] Reference 32. [b] Reference 10. [c] Reference 12. [d] Reference 31. [e] This work, 1.2 equiv of TBDMS-Cl used, base = imidazole. [f] Reference 33. [g] Reference 34.

Table 2. Isolated Yields for the Regioselective Disilylation of Methyl/Phenyl Hexopyranosides with the $PdCl_2$ (3 mol %)/^{t}BuMe$_2$SiH System (Results for ^{t}BuMe$_2$SiCl/Base Method in Parentheses Taken from Halmos et al.[11] unless Indicated Otherwise)

entry	sugar substrate	amount of TBDMS-H (mol equiv) (TBDMS-Cl in parentheses)	yield of 6-position monosilylated derivatives (%)	yield of disilylated derivatives (%) 2,6	3,6	4,6	yield of trisilylated derivatives (%) 2,3,6 and 2,4,6	total yield of silylated sugars (%)
1	methyl α-D-Glu (**1**)	2.4 (2.2)	<5 (2)	18 (70)	63 (11)	5 (−)	3 (9)	89 (92)
		3.3 (3.2)	<5	17 (42)	65 (15)	5 (−)	5 (18)	92 (75)
2	methyl β-D-Glu (**2**)	2.4 (2.2)	<5 (31)	19 (20)	62 (20)	6 (−)	3 (−)	90 (71)
		3.3 (3.2)	<5 (−)	19 (28)	62 (29)	6 (1)	3 (−)	90 (74[a])
3	phenyl β-D-Glu (**3**)	2.4 (2.2[b])	15 (−)	13 (29)	63 (48)	5 (−)	1 (17)	96 (94)
		3.3[c]	20	14	58	5	1	97
4	methyl α-D-Man (**6**)	2.4 (2.2)	23 (−)	9 (50)	62 (33)	1 (5)	− (9)	95 (97)
		3.3 (3.2)	20 (−)	11 (40)	59 (16)	− (−)	− (19)	90 (75)
5	methyl α-D-Gal (**7**)	2.4 (2.2)	8 (−)	36 (66)	39 (21)	− (−)	6 (10)	88 (97)
		3.3 (3.2)	15 (−)	35 (84)	40 (−)	− (−)	3 (14)	92 (98)
6	methyl β-D-Gal (**8**)	2.4 (2.2)	23 (−)	30 (35)	37 (43)	− (−)	2 (8)	92 (86)
		3.3 (3.2)	14 (−)	36 (31[d])	43 (−)	− (−)	3 (49)	96 (80)

[a] Includes some tetrasilylated product. [b] This work. [c] Not determined for TBDMS-Cl. [d] 2,6-/3,6-Isomers not separated by Halmos et al.[11]

metal once all silane had been consumed. The precipitation of the catalysts prevents a direct reuse of the palladium colloid, but the metal can be fully recovered by filtration as the first step of the very simple workup procedure. Concentration of the solvent in vacuo directly gives the silylated sugars, which were then separated into their respective isomers by flash column chromatography or, in a few more difficult cases, by preparative HPLC.

To allow a comparison of the classical silyl chloride with the new silane alcoholysis method for the sugars listed in Chart 1, those substrates (mainly the pentose derivatives) for which no literature data were available were also silylated using TBDMS-Cl/imidazole, closely following the procedure described by Halmos et al.[11] Switching the solvent from *N*,*N*-dimethylformamide (DMF) to DMA had no effect on yields or product distributions.

Six-position monosilylated and disilylated sugars are accessible with the silane alcoholysis method, with the product distributions between the two being primarily dependent on the amount of silane employed. Table 1 gives the conditions for the monosilylation of the six hexopyranosides investigated and compares them to yields achieved by previously published procedures.[10,12,31−34] The monosilylation reactions were empirically optimized by variation of three parameters: reaction temperature, equivalents of silane, and catalyst precursors. In four of the six cases, use of the somewhat less reactive Pd(OAc)$_2$-derived catalyst (vide infra) proved to be the key to limiting the reaction to the 6-monosilylated sugars as the main products. In particular for **1**, the monosilylated product **1a** (see Chart 1 for the numbering scheme) was isolated with this catalyst, even if a large excess of silane was used. In all cases, the remainder of the materials isolated consisted of unreacted starting material and smaller amounts of disilylated sugars, both of which were readily separated from the desired 6-monosilylated material by flash column chromatography. No monosilylated sugars with silylation in a position other than O-6 were observed; i.e., the sterically most accessible primary alcohol function is always silylated first by either method.

When the reactions were carried out with 2 equiv or more of TBDMS-H, the disilylated sugars consistently become the dominant products. Using 3.3 rather than 2.4 equiv of silane had only a minor impact on the overall yields and product distributions, and only very small amounts of trisilylated products were observed. Table 2 summarizes the results of the silane alcoholyis reaction for the six methyl and phenyl pyranosides employed and compares them to those (given in parentheses) obtained by Halmos et al. and ourselves through the classical silyl chloride method. The identity of the isomers was in each case established by ^{1}H-COSY, ^{13}C-JMOD, and ^{1}H/^{13}C-HSQC NMR spectroscopy (see Experimental Section and Supporting Information for exhaustive NMR data and spectra).

The most notable feature of the silane alcoholysis reaction is that for the first four entries in Table 2, i.e., the glucose derivatives **1**−**3** and the mannose derivative **6**, the product distributions of 2,6- and 3,6-disilylated sugars are complementary to those obtained through the silyl chloride/imidazole method—for the former the 3,6- and for the latter the 2,6-disilylated pyranoside is the main product. A regioselective 3,6-silylation of **6** was also achieved by Halmos et al.[11] by using a combination of triethylamine and *N*,*N*′-dimethyl-4-aminopyri-

(31) Brandstetter, H. H. v.; Zribal, E. *Helv. Chim. Acta* **1980**, *63*, 327−343.
(32) Johnson, D. V.; Taubner, L. M. *Tetrahedron Lett.* **1996**, *137*, 605−608.
(33) Mark, E.; Zbiral, E.; Brandstetter, H. H. *Monatsh. Chem.* **1980**, *111*, 289−307.
(34) Villalobos, A.; Danishefsky, S. J. *J. Org. Chem.* **1990**, *55*, 2776.

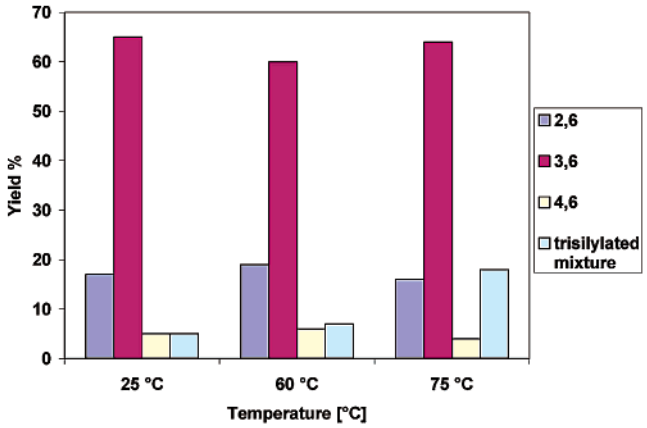

Figure 1. Product distribution and yields of the silylation of methyl α-D-glucopyranoside (**1**) with the TDBMS-H/$PdCl_2$ system as a function of temperature.

dine (DMAP) instead of imidazole as the base. Through control reactions they established that for this sugar the initial product is, in fact, the 3,6-silylated isomer, which under the imidazole reaction conditions isomerizes to the 2,6-silylated isomer, a process that the authors relate to the cis relationship of the OH-2 and OH-3 groups in **6**. In the presence of NEt_3/DMAP, the isomerization is suppressed, and **6b** is obtained as the main product. Under the same conditions (i.e., NEt_3/DMAP/TBDMS-Cl), Halmos and co-workers reported that for the glucose and galactose substrates **1**, **2**, **7**, and **8**, both the 2,6- and 3,6-isomers are formed in ∼40% yield in each case; i.e., essentially no regioselectivity and also no isomerization was observed. Control experiments under our base-free silane alcoholysis conditions also showed no isomerization for any of the sugars, including **6b** and **6c**. Applying the silane alcoholysis method to the two methyl D-galactopyranosides **7** and **8** (entries 5 and 6 in Table 2), the 3,6-isomers were still the more abundant products formed; however, the regioselectivity bias of 3,6 over 2,6 was only marginal (≤7%) and only for sugar **7** exceeds the yield of 3,6-isomer obtainable through the silyl chloride method. With all other parameters unchanged, the much diminished relative regioselectivity for either silylation method must therefore be a consequence of the axial orientation of OH-4 in the galactose-derived substrates.

With **1** as the model compound and $PdCl_2$ as the catalyst precursor, we also tested the temperature dependence of regioisomer distribution and overall yield. As Figure 1 shows, the only notable effect of raising the temperature from 25 to 60 or 75 °C was a slight increase in the amount of trisilylated sugar, while the other isolated yields varied only within estimated the error range of the isolation procedure (≤5%).

We hypothesized that steric interactions between the 6-OTBDMS and/or the anomeric methyl group on the sugar and either the active silylation species in the TBDMS-Cl/base system (most likely $[TBDMS\text{-}base]^+$) or the palladium metal surface in the TBDMSH/Pd(0) system could be origin of the observed differences in regioselectivity between the two methods, which should thus disappear if these interactions could not occur. We therefore carried out a comparative study of the effect of the presence of the 6-OTBDMS and anomeric substituents on any regioselectivities in the silylation of the three secondary ring hydroxyl functions using the two series methyl β-D-glucopyranoside (**2**) → methyl β-D-xylopyranoside (**4**) → 1,5-anhydro-xylitol (**5**) and methyl α-D-galactopyranoside (**7**) → methyl β-D-arabinopyranoside (**9**) → 1,5-anhydro-arabinitol (**10**). The second series is valid, because arabinose is known to exist primarily in the $^1C_4$ conformation.[1] Methyl β-L-arabinopyranoside is then formally derived from methyl α-D-galactopyranoside by replacing the 6-CH_2OH function with hydrogen. Since all other reagents are nonchiral, the enantiomeric relationship between this enantiomer and the actually employed methyl β-D-arabinopyranoside is irrelevant for the purpose of this study. Figure 2 clarifies this stereochemical relationship.

Table 3 summarizes the results of silylations by both methods for the two series. The first three entries show a clear preference for 3-silylation by the silane alcoholysis method, while the silyl chloride method gave mixtures of the 2- and 4-silylated sugar as the main product. In fact, for **9** the preference for 3-silylation is much higher than for the parent compound **7** in the galactose-derived series (see entry 5 in Table 2). The 2- and 4-silylated sugars **5b** and **5d** are enantiomers to each other and thus cannot be separated by conventional chromatography. Preparative HPLC allowed us to separate the other 2- and 4-silylated sugars **4b** and **4d** and **9b** and **9d**, respectively, and unambiguously assign their structures by NMR spectroscopy. Unfortunately, we were not able to separate compounds **10a**−**c** by HPLC or other chromatography techniques, leaving the comparison incomplete for the second series of sugars. The NMR spectrum of the isomeric mixture of **10** is too complex for meaningful

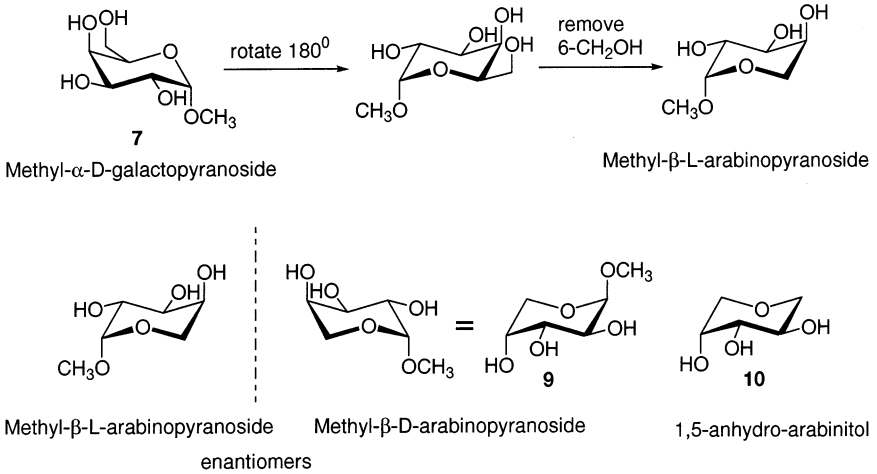

Figure 2. Stereochemical relationship between methyl α-D-galactopyranoside (**7**) and methyl β-D-arabinopyranoside (**9**).

Table 3. Effect of the Removal of 6-CH_2OH and the Anomeric Substituents on the Product Distribution for Glucose and Galactose Derivative: Silylation with 1.2 Equiv of TBDMS-H/-Cl (Isolated Yields from the $^tBuMe_2SiCl$/Imidazole Method (This Work) in Parentheses)

		monosilylated derivatives (%)			
entry	sugar substrate	**2** + **4**[a]	**3**	disilylated derivatives (%)	total silylated compounds (%)
1	methyl β-D-Xyl (**4**)	20 [10 + 10]	57	4	81
		(42 [14 + 28])	(29)	(16)	(87)
2	1,5-anhydro-Xyl (**5**)	23 (racem.)	44	18	85
		(41)	(23)	(20)	(84)
3	methyl β-D-Ara (**9**)	27 [22 + 5]	43	12	82
		(54 [36 + 18])	(9)	(18)	(81)
4	1,5-anhydro-Ara (**10**)	34; 1.1:1.0:0.8 mixture of three inseparable isomers		8	42
		(25; 0.3:0.9:1.0 mixture of three inseparable isomers)		(38)	(63)

[a] Separated by prep. HPLC.

isomer assignments, and only the relative ratio of isomers could be extracted from the data. Nevertheless, the sum of these experiments leads us to conclude that steric interactions due to the presence of 6-OTBDMS and/or the anomeric methyl group cannot explain the observed differences in regioselectivity between the two methods.

A second hypothesis is that the observed differences in regioselectivities may reflect a kinetic vs thermodynamic product distribution, with the uncatalyzed silyl chloride reaction giving a thermodynamic and the palladium-catalyzed silane alcoholysis reaction giving a kinetic product distribution. If this were true, and taking into account that our control experiments established that no isomerization takes place under the silane alcoholysis conditions, reacting a 6-silylated sugar substrate with less than 1 equiv of TBDMS-H should yield exclusively the 3,6-silylated product. Table 4 shows the results of this experiment for methyl α-D-glucopyranoside (**1**) as the model compound. The ratio of **1c**/**1b** isolated is very similar, whether 0.3 or 1.2 equiv of silane was used, suggesting that the two isomers were formed simultaneously at approximately equal rates; i.e., on the basis of this experiment, one cannot assign a kinetic or thermodynamic preference to either one of them.

Table 4. Product Distribution in the Pd(0) Nanoparticle-Catalyzed Reaction of 6-*tert*-Butyldimethylsilyl-methyl-α-D-glucopyranoside with 0.3 and 1.2 Equiv of TBDMS-H

amount of	yields of disilylated sugars (%)			ratio	yield of recovered
TBDMS-H used (equiv)	2,6	3,6	4,6	3,6/2,6	starting material (%)
0.3	2.5	7.5	<1	3.0	85
1.2	15	53	4	3.5	10

To further test this notion, we determined the equilibrium constants of the hypothetical isodesmic isomerization reaction defined in Figure 3 for the methyl D-pyranosides **1**, **4**, **6**, **7**, and **9** by calculating their total energies and applying the van't Hoff's equation. The energies in Table 5 were calculated ab initio at the HF/3-21G* level and include zero-point and thermal free energy corrections. No imaginary frequencies were observed in the calculations. The differences in free enthalpy between the silylation isomers are very small (less than 5 *RT*), and the resulting equilibrium constants cluster very closely around unity. The energies and resulting equilibrium constants in Table 5 were calculated in vacuo, i.e., ignoring solvent effects. For the glucose- and galactose-derived isomers, lying at the opposite extremes of calculated $\Delta\Delta G$ values, we therefore recalculated the energies, taking the presence of DMA solvent into account through a continuum model ($\epsilon_{DMA} = 37.78$, $a_0 = 6.10-6.29$).[35−37] Within the continuum model, the influence of the solvent is marginal, with energy differences of 3.376 and −1.556 kcal/mol for the **1b**/**1c** and **7b**/**7c** pairs, respectively, resulting in the equilibrium constants given in the last column of Table 5, which are also essentially unity. We cannot exclude the possibility that, in a specific solvation model, larger energy differences between the respective isomers might emerge; however, we would anticipate them to be small, given the small differences in topology between the disilylated isomers. Also, such a specific model would require the consideration of defined orientations and hydrogen bonds between the sugar substrate and an unknown number of DMA molecules in the first and possibly second solvation sphere of each isomer, which constitutes an enormous challenge beyond our present computational abilities. In summary, the calculations suggest that the observed regioselectivities do not reflect intrinsic thermodynamic and kinetic product distributions, but under the reaction conditions are a function of the silylation agent alone rather than the substrate.

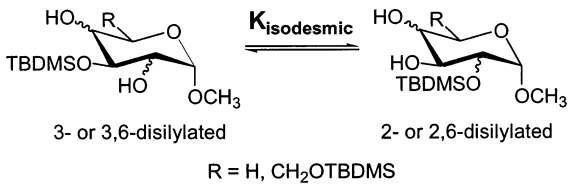

Figure 3. Isodesmic isomerization reaction between 2-/2,6- and 3-/3,6-silylated methyl α-D-pyranosides.

Using both Ph_3SiH and TBDMS-H as the silane, we also applied our method to the conformationally locked sugar derivatives 1,6-anhydro-β-glucopyranoside and 1,3,5-*O*-methylidene-*myo*-inositol. Table 6 summarizes the results of these experiments. With the exception of the 2-silylated and 2,4-disilylated inositols of entry 1,[38] all compounds in Table 6 are new. Most significantly, the silane alcoholysis method gives access to the racemic 4-TBDMS-1,3,5-*O*-methylidene-*myo*-inositol in ∼40% yield. This substitution pattern has, to our knowledge, previously not been achieved on this sugar and may be of high synthetic value in the preparation of selectively phosphorylated inositols, which play an important biological role in cell membranes and as secondary messengers.

With Ph_3SiH as the silane, the addition of 2 equiv of Proton Sponge (1,8-bis(dimethylamino)naphthalene) per palladium results in higher yields, as the base scavenges HCl generated

(35) Kirkwood, J. G. *J. Chem. Phys.* **1934**, *2*, 351.
(36) Onsager, L. *J. Am. Chem. Soc.* **1936**, *58*, 1486−1493.
(37) Wong, M. W.; Frisch, M. J.; Wiberg, K. B. *J. Am. Chem. Soc.* **1991**, *113*, 4776−4782.
(38) Angyal, S. J. *Carbohydr. Res.* **2000**, *325*, 313−320.

Table 5. Total Energies of and Energy Differences and Resulting Equilibrium Constants for the Isodesmic Isomerization Reaction between 2-/2,6- and 3-/3,6-Silylated Methyl D-Pyranosides **1**, **4**, **6**, **7**, and **9** Calculated at the HF/3-21G* Level[a]

silylated sugar	total free energy ΔG[b] (kcal/mol)	$\Delta\Delta G$[c] (kcal/mol)	K_{iso} at 298 K[d]	solvent-corrected K_{iso} at 298 K
2,6-di-TBDMS-methyl-α-D-Glu (**1b**)	−1105145.36	2.8458	0.9952	0.9943
3,6-di-TBDMS-methyl-α-D-Glu (**1c**)	−1105148.20			
2-TBDMS-methyl-β-D-Xyl (**4b**)	−633828.78	0.2868	0.9995	n.d.
3-TBDMS-methyl-β-D-Xyl (**4c**)	−633829.07			
2,6-di-TBDMS-methyl-α-D-Man (**6b**)	−1105142.76	−0.4424	1.0007	n.d.
3,6-di-TBDMS-methyl-α-D-Man (**6c**)	−1105142.32			
2,6-di-TBDMS-methyl-α-D-Gal (**7b**)	−1105150.92	−2.8494	1.0048	1.0026
3,6-di-TBDMS-methyl-α-D-Gal (**7c**)	−1105148.07			
2-TBDMS-methyl-β-D-Ara (**9b**)	−633827.71	−1.5964	1.0027	n.d.
3-TBDMS-methyl-β-D-Ara (**9c**)	−633829.07			

[a] In vacuo. [b] Energies in hartrees were calculated to five decimal places with nine significant digits and are converted to kcal/mol by multiplying with 627.51 kcal/a.u. and rounded in this table. [c] $= \Delta G$(2-/2,6-) − ΔG(3-/3,6-). [d] By $K = e^{-\Delta G/RT}$.

Table 6. Silylation of 1,6-Anhydro-β-glucopyranoside and 1,3,5-*O*-Methylidene-*myo*-inositol with TBDMS-H or Ph_3SiH and 3 mol % $PdCl_2$ at 60 °C (Isolated Yields from the ^{t}BuMe$_2$SiCl/Base Method in Parentheses)[a]

				monosilylated derivatives (%)			
entry	sugar substrate	silane	amount of silane (equiv)	**2-eq.**	**4-ax.**	2,4-disilylated derivatives (%)	total yield (%)
1	1,3,5-*O*-methylidene-Inositol (**12**)	TBDMS-H	1.2 (1.0)	6 (74)	38 (rac.) (−)	37 (rac.) (−)	81 (74)[a]
2	1,3,5-*O*-methylidene-Inositol (**12**)	TBDMS-H	2.4	−	39 (rac.)	52 (rac.)	91
3	1,3,5-*O*-methylidene-Inositol (**12**)	Ph_3SiH[b]	2.3		−	57 (rac.)	57
4	β-1,6-anhydro-glucopyranose (**11**)	Ph_3SiH[b]	2.3		−	90	90

[a] Reference 38; base employed is 2,6-lutidine. [b] Two equivalents of Proton Sponge with respect to $PdCl_2$ added.

during the in situ generation of the Pd(0) catalyst (vide infra), which otherwise leads to some loss of silane from the product.

Nature of the Catalyst. In their seminal work, Sommer and Lyons found that, in methylene chloride, xylene, or pentane solvent, palladium supported on charcoal, palladium metal itself, and bulk palladium metal, generated in situ from $PdCl_2$ and various trialkyl silanes as the reducing agent, all form active catalysts.[28] Employing optically active silanes, Sommer and Lyons also established that, for the first two of these catalysts, the alcoholysis proceeds with inversion of stereochemistry at the silicon, while for the third the reaction leads to racemic products, which they attributed to the presence of an acidic racemizing agent, most likely HCl. When the catalyst is moderated by the presence of small amounts of NEt_3, complete inversion of the silane is again observed. In both cases, the authors note that bulk palladium metal immediately precipitates from the solution to form the active catalyst.

We observed the same behavior when using either methylene chloride or acetonitrile as the solvent; however, the resulting palladium metal was not active or was only marginally active for the further silylation of secondary hydroxyl functions in 6-TBDMS-methyl-α-D-glucopyranoside, a sugar substrate soluble in these solvents. In contrast, we found that the addition of TBDMS-H to PdX_2 ($X = Cl^-$, OAc^-) suspended in DMA solvent did not lead to the precipitation of bulk metal. Instead, black solutions of homogeneous appearance were formed, which in the presence of excess silane are catalytically highly active for the silylation of DMA soluble sugars and stable for months with no precipitation of agglomerates of palladium metal, even when stored at − 20 °C.

Prompted by earlier reports by Fowley et al.[39] and Reetz et al.[40,41] that described the formation of palladium colloids either by the reaction of homogeneous solutions of Pd(hfacac)$_2$ (hfacac = $CF_3COCHCOCF_3$) in heptane, diethyl ether, methylene chloride, or acetone with Et_3SiH and other silanes or by the reaction of $Pd(OAc)_2$ in the same solvent (DMA) using an excess of NaOAc as the reducing agent, respectively, we suspected that the catalytically active black solutions generated with silane in DMA may, in fact, also represent a palladium colloid, and we decided to characterize it in detail by dynamic light scattering (DLS) and transmission electron microscopy (TEM).

Table 7. Results of the Characterization of the Palladium Colloids by TEM and DLS

	catalyst precursor			
			$Pd(OAc)_2$	
	$PdCl_2$	$Pd(OAc)_2$	large	small
TEM data				
no. of particles sampled	100	213	88	80
temperature (°C)	25	25	60	
mean size (nm)	**2.04**	**62.21**	**25.66**	**3.16**
ESD	0.57	33.74	6.02	0.64
min. size (nm)	1.03	21.83	12.75	1.97
max. size (nm)	3.4	207.71	42.69	5.2
DLS data				
mean size (nm)	**1.83**	**44.8**	**2.46**	

Table 7 summarizes the results of the TEM and DLS analysis of three representative colloids formed from $PdCl_2$ at 25 °C and from $Pd(OAc)_2$ at 25 and 60 °C in the presence of a 40-fold excess of TBDMS-H. The particle size distributions were reproducible within the error ranges indicated in the table. TEM images of three representative samples formed under these conditions are shown in Figure 4. From the data, the size of particles formed is a function of the counterion and temperature. With the chloride counterion, a nanoparticle colloid of very small particles and narrow size distribution was obtained. Figure 5 directly compares the size distribution measured for this

(39) Fowley, L. A.; Michos, D.; Luo, X.-L.; Crabtree, R. H. *Tetrahedron Lett.* **1993**, *34*, 3075−3078.
(40) Reetz, M. T.; Maase, M. *Adv. Mater.* **1999**, *11*, 773−777.
(41) Reetz, M. T.; Westermann, E. *Angew. Chem., Int. Ed.* **2000**, *39*, 165−168.

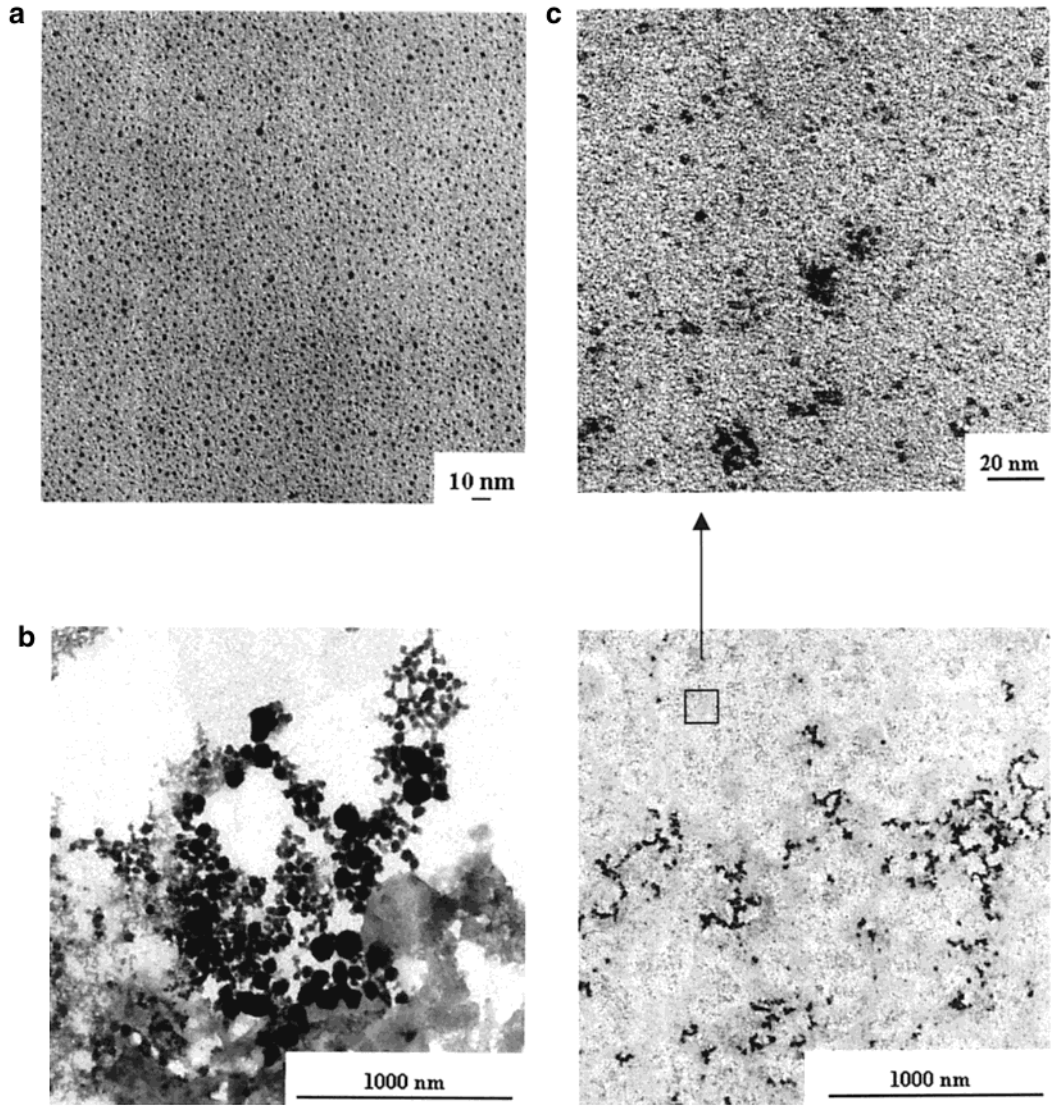

Figure 4. (a) TEM image of a colloid formed from $PdCl_2$ at 25 °C. (b) TEM image of a colloid formed from $Pd(OAc)_2$ at 25 °C. (c) TEM images of a colloid formed from $Pd(OAc)_2$ at 60 °C. Representative smaller particles on top, larger ones at bottom. The top image is a direct enlargement of a section of the lower one.

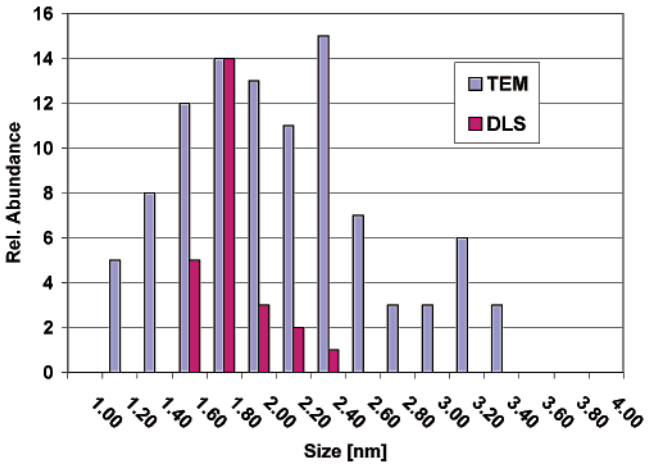

Figure 5. Comparison of particle size distributions obtained by TEM and DLS in a Pd(0) colloid generated from $PdCl_2$/TBDMS-H at 25 °C in DMA.

colloid by TEM with those resulting from DLS. Since DLS allows catalyst characterization under the same conditions as the actual reaction, the excellent agreement between the two data sets indicates that the appearance of the TEM images is not an artifact of the sample preparation, but a genuine representation of the catalyst colloid in solution. When $Pd(OAc)_2$ was used as the colloid precursor at room temperature, much larger particles, as shown in Figure 4b, with a much wider size distribution were obtained, in which most of the larger particles visually appear to be agglomerates of smaller ones of 20−40 nm diameter. At 60 °C, $Pd(OAc)_2$ resulted in a colloid that showed a bimodal particle size distribution, with the smaller particles, shown in the enlarged section of Figure 4c, by TEM being close in size to those formed from $PdCl_2$. The DLS results for the acetate-derived colloid formed at room temperature do not show good agreement with the TEM data, which, as already pointed out by Watzky and Finke,[42] illustrates the fact that DLS is essentially a statistical method that gives reliable results only for monodisperse sets of particles. A much better agreement of the DLS with the TEM data is observed for the acetate-derived colloid formed at 60 °C, as its DLS behavior is dominated by the much more abundant smaller particles.

(42) Watzky, M. A.; Finke, R. G. *J. Am. Chem. Soc.* **1997**, *119*, 10382−10400.

Scheme 1

Pd^0 catalyzed chloride dependent silylation:

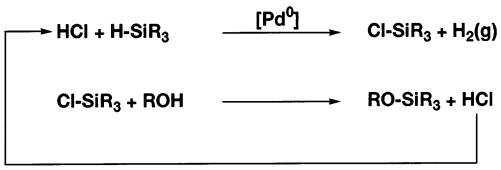

The different particle sizes with different counterions under otherwise identical conditions point to different nucleation and/or growth rates as a function of the counterion present. In this context, the fact that the colloid is stable only as long as free silane is present suggests that the silane rather than the counterions stabilize the colloid against agglomeration. A more detailed study of the palladium colloid that addresses its mechanism of formation and stabilization as well as the elemental composition and surface structure of the nanoparticles will be presented elsewhere.

Finally, there is a qualitative correlation between the particle size and the observed catalytic activity; i.e., the colloid formed from $PdCl_2$ at 25 °C is much more active than that formed from $Pd(OAc)_2$ at the same temperature. In turn, the colloid formed at 60 °C from $Pd(OAc)_2$, containing particles close in size to those of the $PdCl_2$-derived colloid, showed a comparable, only slightly lower catalytic activity. Combined with the observation that bulk palladium metal is essentially inactive for the silylation of sugars, this suggests that it is primarily the available surface area that determines the overall catalytic activity.

Discussion

Possible Reaction Mechanisms and Origin of the Regioselectivity in the Sugar Silylations. In a control experiment, we found that powdered palladium black could be activated in situ by a small amount of TBDMS-Cl (equimolar to palladium) to give a moderately active silane alcoholysis catalyst, which however did not show colloid formation. Together with the initial observation that powdered palladium metal did not show catalytic activity for the silylation of the sugar substrates, this hinted that, with the $PdCl_2$-generated colloids, chloride might play an active role in the silane alcoholysis. In particular, we considered the possibility that TBDMS-Cl might be formed catalytically in a low *steady-state* concentration at the palladium surface and constitute the actual reactive species, and that the reaction could follow the path presented in Scheme 1.

Since the mechanism in Scheme 1 requires the transient presence of free HCl, it should be inhibited by the addition of a base. We therefore also conducted silane alcoholysis reactions with **1** as the model substrate in the presence of 2 equiv (with respect to $PdCl_2$) of Proton Sponge or DABCO (1,4-diazabicyclo-[2.2.2]octane). In the presence of the first base, the reactions had to be heated to 60 °C in order to achieve a catalytic silylation, and the isolated yields of **1b** and **1c** were somewhat lower, at 16% and 47%, respectively (compare with the yields in Table 2), while in the presence of DABCO only 6-monosilylated products were found; i.e., base inhibited the reaction.

However, the reaction also proceeded with $Pd(OAc)_2$, for which an HOAc-mediated catalytic cycle analogous to Scheme 1 is unlikely, as the silicon−oxygen bond in TBDMS-OAc is unreactive against alcohols once formed due to its high bond energy. Also, the product distribution of regioisomers in the sugar products obtained by silane alcoholysis was not affected by the type of catalyst precursor; e.g., the silylation of methyl α-D-glucopyranoside with $Pd(OAc)_2$-derived colloids gives, within error range (±3%), the same yields and regioisomer distribution as the reaction with a $PdCl_2$-derived catalyst if the reaction temperature is raised to 60 °C in order to compensate for the slightly lower activity of the acetate colloid. This leads us to conclude that TBDMS-Cl cannot be the active silylation species and that the activation of palladium black by small amounts of TBDMS-Cl must be a surface activation effect, possibly the removal of an oxide coating of the palladium powder by the thermodynamically favorable formation of silicon−oxygen bonds. The lower reactivity of the catalyst in the presence of base is then a consequence of the adsorption of the base or its protonated form to the palladium surface. DABCO should show stronger adsorption than the Proton Sponge due to its more rigid structure and the more pronounced directionality of the free electron pair on nitrogen. This interpretation is consistent with Reetz's observation of a monolayered coating of palladium nanoparticles by tetraalkylammonium salts.[43]

In light of the results of the calculations (see Table 5), the different regioisomer distributions realized by the two different silylation methods are not intrinsically related to the sugar structure but are a consequence of different modes of interaction between the sugar and either the heterogeneous palladium/solution interface in the silane alcoholysis reaction or the active silylation reagent derived from silyl chlorides and base, most likely of the type $[R_3Si{-}NR_3']^+$ in molecular disperse homogeneous solution.

For the silyl chloride method, we considered two possible origins for the observed regioselectivities: chelation of a hypervalent silicon in the transition state of the reaction by cis-related hydroxyl functions in the sugars or activation of individual hydroxyl functions toward electrophilic attack by $[R_3Si\text{-}NR_3]^+$ through intramolecular hydrogen bonds. As shown in Figure 6, a chelation of the postulated silylating agent $[R_3Si\text{-}NR'_3]^+$, here formulated as a six-coordinate transition state, should be possible between any cis-related hydroxyl functions. Eliminating the protonated base $[HNR'_3]^+$, analogous five-coordinate intermediates as local minima along the reaction coordinate could also be formulated. In either case, the hydroxyl groups involved are the OH-2 and OCH_3-1 oxygens for methyl α-D-gluco- and galactopyranosides, OH-2 and OH-3 for methyl α-D-mannopyranoside, the OCH_3-1 and OH-2 in methyl β-D-arabinopyranoside, and also the OH-4 and OH-3 in the galactopyranosides. A chelation with one or both ring oxygens could also explain the high preference for 2-silylation in the inositol derivative **12** with TBDMS-Cl, while for any conceivable trans-1,2-diequatorial diol units such a chelation appears less likely. The notion of a chelation-controlled regioselectivity correlates well with the observed isomer yields in Tables 2 and 3. The substrates **2**, **3**, **4**, **5**, and **8**, in which no chelation involving OH-2 is expected, show much less preference for the 2-/2,6- over the 3-/3,6-isomer, typically less than 10%, while for substrates **1**, **6**, **7**, and **9** that can chelate through OH-2, the 2,6-isomer dominates. An overall higher reactivity of OH-2 against electrophilic attack by benzoyl and methylsulfonyl

(43) Reetz, M. T.; Helbig, W.; Quaiser, S. A.; Stimming, U.; Breuer, N.; Vogel, R. *Science* **1995**, *267*, 367−369.

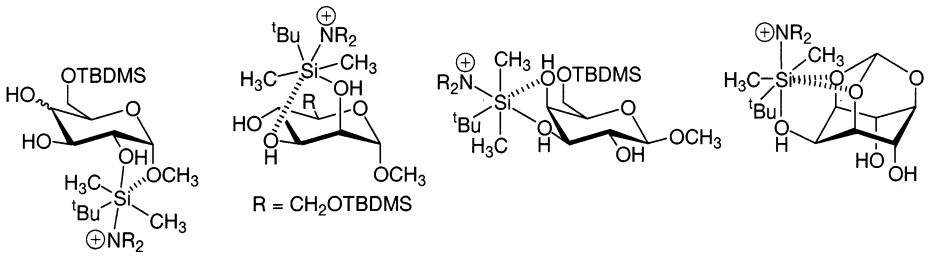

Figure 6. Possible induction of regioselectivity by hypervalent silicon chelation in the transition state of the $^{t}BuMe_2SiCl$/base method.

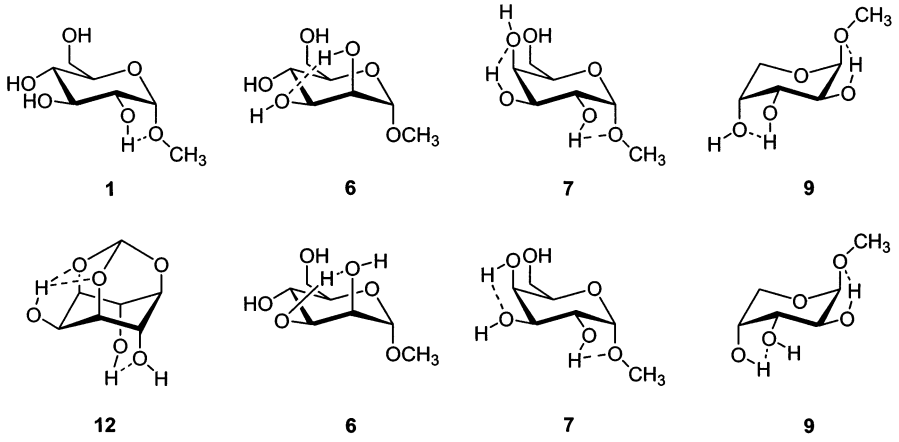

Figure 7. Possible intramolecular hydrogen bonding between cis-related hydroxyl functions in pyranosides **1**−**12**.

groups has previously also been observed for gluco- and galactopyranosides, while for mannopyranosides OH-3 was most reactive.[44] As mentioned earlier, Halmos et al.[11] found that, depending on the base employed, either the 2,6-silylated (**6b**) or 3,6-silylated mannose derivative (**6c**) is formed, with the latter isomerizing to the former in an imidazole/DMF mixture, but not in triethylamine/DMF. This observation suggests that, at least for **6**, specific hydrogen bonding between the substrate and the various solvent/base combinations employed create large enough energy differences between the isomers to distinguish kinetic and thermodynamic products, overlaying the very small energy differences presented in Table 5.

A specific solvation of the substrate through hydrogen bonds between the sugar and the solvent and its impact on intramolecular hydrogen bonds in the substrate could thus also explain the observed regioselectivities. Intramolecular hydrogen bonds in sugars are weak, typically on the order of 1−3 *RT* (i.e., less than 1.8 kcal/mol), but are well established by ^{1}H NMR studies, even in DMSO-d_6, which is even more polar ($\epsilon = 48.9$) than DMA ($\epsilon = 37.78$)[45−47] and have also been proposed on the basis of solution-state IR[48,49] and theoretical studies.[50] Intramolecular hydrogen bonds are also inferred to be the origin of regioselectivity in the DMAP-catalyzed acetylation of octyl hexopyranosides in $CHCl_3$.[51] A SIMPLE NMR study by Angyal and Christofides[46] concluded that, at room temperature and any given time, only 5−10% of a dissolved sugar will have intramolecular hydrogen bonds, reflecting competition from binding to the solvent and the fact that their relative energies are on the order of thermal motion in the system, i.e., *RT*. Following the Curtin−Hammett principle, the low abundance of intramolecularly bonded hydroxyls is, however, irrelevant, provided they react faster than nonbonded ones. This would indeed be expected for oxygen atoms in hydroxyl functions that act as proton donors in hydrogen bonds and that should therefore display an enhanced nucleophilicity.

Possible modes of activation of individual hydroxyl functions by intramolecular hydrogen bonding in the substrates **1**, **6**, **7**, **9**, and **12** are shown in Figure 7. Analogous to the alternative chelation model, the structures in Figure 7 assume that effective hydrogen bonding is possible only between cis-related hydroxyl functions; e.g., a hydrogen bond is likely to occur between the OH-2 and the oxygen in OCH_3-1 in the α-forms of gluco- and galactopyranoside, but not in the β-forms. For each of the sugars **6**, **7**, and **9**, two hydrogen bond orientations are conceivable and shown in Figure 7, leading to a nucleophilic activation of either O-2 or O-3 in **6**, or O-3 or O-4 in **7** and **9**, respectively. The α/β-pairs of sugars **1**/**2** and **7**/**8** provide a direct test of the hydrogen-bonding model: For both pairs, the yields in Table 2 show that there is a strong preference of 2-silylation by silyl chloride for the α-form, but essentially no selectivity for the β-form. The latter is also true for the phenyl β-glucopyranoside **3**. The preference for 2-silylation in **6** and **9** suggests that the hydrogen-bond-activating OH-2 (top row in Figure 7) may be more prevalent. For the xylose substrates **4** and **5**, no hydrogen bond influence is expected due to the all-trans orientation of the hydroxyl functions. In **4**, positions 3 and 4 are preferentially silylated, possibly reflecting steric hindrance by the anomeric methyl group. Effectively no regioselectivity is observed with **5**, in which the symmetry-equivalent positions 2 and 4 and the

(44) Haines, A. H. *Adv. Carbohydr. Chem.* **1976**, *3*, 11−110.
(45) Christofides, J. C.; Davies, D. B. *J. Chem. Soc., Perkin Trans. 2* **1987**, 97−102.
(46) Angyal, S. J.; Christofides, J. C. *J. Chem. Soc., Perkin Trans. 2* **1996**, 1485−1491.
(47) Bernet, B.; Vasella, A. *Helv. Chim. Acta* **2000**, *83*, 995−1021.
(48) Bartsch, J.; Prey, V. *Liebigs Ann. Chem.* **1968**, *717*, 198−204.
(49) Zhbankov, R. G. *J. Mol. Struct.* **1992**, *270*, 523−539.
(50) Woods, R. J.; Szarek, W. A.; Smith, V. H. *J. Am. Chem. Soc.* **1990**, *112*, 4732−4741.
(51) Kurahashi, T.; Mizutani, T.; Yoshida, J.-I. *J. Chem. Soc., Perkin Trans. 1* **1999**, 465−473.

position 3 are, within error range, all silylated in just over 20% yield. The data are incomplete for **10** due to the separation problems noted above. In the inositol derivative **12**, the intramolecular hydrogen bond between OH-2 and the adjacent ring oxygens indicated in Figure 7 may be the cause of the high selectivity for 2-silylation in this substrate.

A rational explanation for the origin of the observed 3-/3,6-preference with the silane alcoholysis method is much more elusive. Because the reaction occurs on the surface of palladium nanoparticles at active sites of presently unknown structure and elemental composition, it is exceedingly difficult to gain further meaningful mechanistic insights, in particular with respect to the observed regioselectivities of the sugar silylations. It is, however, reasonable to postulate that the same silane activation mechanism operates on the nanoparticles as on bulk palladium catalyst. As originally proposed by Sommer and Lyons,[52] a "backside" attack of the alcohol nucleophile on a silane activated by either dissociative or nondissociative chemisorption onto the surface leads to silicon−oxygen bond formation with inversion at the silicon, as proven for chiral silanes by these authors.

There is a strong correlation between the position of ring oxygens and the preferentially silylated hydroxyl function: With the exception of galactose, it is the secondary hydroxyl function most spatially remote from the ring oxygens in the sugar substrates, i.e., OH-3 in the pyranoses and one of the axial hydroxyls in **12** (i.e., OH-4), that is most reactive in the silane alcoholysis reaction. One conceivable explanation is that the sugar preferably reacts out of an orientation that positions the ring oxygen as far away as possible from the palladium surface, which automatically orients OH-3 toward the surface. The effect could therefore originate from an electrostatic repulsion between the nonbonding electron density on the ring oxygens and the palladium surface. The preferential silylation of OH-3 by the Pd(0)/silane system occurs regardless of the presence of an anomeric methyl group and C-6 but appears to be modulated by their presence, possibly due to steric influences. Removing C-6 (see results in Tables 2 and 3) increases the preference for silylation of OH-3 vs OH-2 from 3.3:1 in **2** to 5.7:1 in **4** and from essentially no preference with a ratio of 1:1.1 in **7** to 1:2 in **9**. All these considerations, however, still fail to give a rational explanation for the lack of selectivity observed with the galactose substrates **7** and **8**, and the nature of the effect of the axial hydroxyl OH-4 is unclear.

An electrostatic repulsion between ring oxygens and the catalyst surface can also explain the preference for axial 4-silylation of the inositol deriative **12**, but this result could also be due to steric interactions between the methylidene bridge and the silane-coated palladium surface.

Finally, as with the silyl chloride method, a specific solvation of the sugar, in which the nucleophilicity of individual hydroxyl functions is enhanced by hydrogen bonding, is conceivable, with the presence of the solid/liquid interface imposing a different near-order on the solvent spheres around the sugar molecules than in the silyl chloride method that could then result in the observed different regioslectivities.

Conclusion

The palladium(0) nanoparticle-catalyzed silylation of sugars by silane alcoholysis of TBDMS-H is an attractive alternative to the established silyl chloride method. The nanoparticle nature of the catalysts is a prerequisite for the high catalytic activity observed. In several cases, the new method gives convenient access to isomers that are formed either only as minor components or not at all by the silyl chloride method. Studies to extend the method to disilanes and to explore its tolerance to the presence of various functional groups in the sugar are presently under way.

Experimental Section

General. All synthetic experiments were performed under a dry argon atmosphere by standard Schlenk-tube techniques. Sample solutions for dynamic light scattering (DLS) and transmission electron microscopy (TEM) were prepared inside an inert-gas drybox under argon atmosphere.

Electron microscopy was carried out on a LEO 912AB operating at 100 kV with a liquid nitrogen anticontaminator in place. Digital images were collected using a 1K × 1K PROSCAN CCD camera and processed using the measurement software in the SIS EsiVision program. Both negatively stained (using 2% w/v uranyl acetate) and unstained samples were imaged for measurement comparison. All figures in this paper are of unstained samples, so that the region of electron density in each particle is attributed to the palladium.

Dynamic light scattering (DLS) was used to determine the size distributions of the suspended colloids prepared as described below. For each run, 100 μL of concentrated palladium colloidal suspension was transferred to a square (optics quality) cuvette (QS, Hellma, Concord, ON) containing 4 mL of the appropriate solvent. Incident light (of wavelength 532 nm) was provided by a 50 mW Nd:YAG laser (DPSS 532, Coherent, Santa Clara, CA), and light scattered at 90° was correlated using a BI9000AT autocorrelator (Brookhaven Instruments Corp., Holtsville, NY) with software 9KDLSW Ver.1.35. Correlation function analysis was performed to obtain number distributions that could be compared to data obtained from electron microscopy. A detailed description of the program TRIMIE (compiled using Lahey F95, Incline Village, NV) used for this task has been described by Hallett et al.[53] Input parameters for solvent viscosity and refractive index were 2.141 cP and 1.438, respectively, obtained from the *CRC Handbook of Chemistry and Physics*.

NMR spectra were recorded on Bruker Avance 400 and 600 MHz instruments in deuterated solvents obtained from CIL Inc. Isomer assignments of the silylated sugar species were made on the basis of 2D COSY, NOESY, and HSQC spectra (see Supporting Information for details). Elemental analyses were performed by M-H-W Laboratories, Phoenix, AZ. Sugar substrates, ^{t}BuMe$_2$SiH, and metal salts were purchased from Aldrich Chemical Co. and Strem Chemicals, respectively, and used as received. 1,5-Anhydro-xylitol and 1,5-anhydro-arabinitol were prepared according to literature procedures.[54] Methyl β-D-arabinopyranoside was prepared by Fischer glycosidation with methanol and purified by recrystallization from ethanol/ethyl acetate. *N*,*N*-Dimethylacetamide (DMA) and *N*,*N*-dimethylformamide (DMF) were obtained from Caledon Laboratories Ltd. or Fisher Scientific, dried by vacuum distillation from BaO, and subsequently stored over activated 4 Å molecular sieves. Flash column chromatography was performed on wet-packed Merck silica gel 60F at 1 psi static pressure, set by a break-through valve at the column head. HPLC separations were performed on a Varian ProStar system fitted with UV and RI detectors using 41 × 250 mm columns. Details for the chromatographic separations of the individual sugars are given in the Supporting Information.

General Procedure for the Silylation of Sugar Substrates Using PdX_2 (X = Cl^-, OAc^-) as Catalyst Precursors. A DMA (3 mL)

(52) Sommer, L. H.; Lyons, J. E. *J. Am. Chem. Soc.* **1967**, *89*, 1521−1522.

(53) Hallett, F. R.; Craig, T.; Marsh, J.; Nickel, B. G. *Can. J. Spectrosc.* **1989**, *34*, 63−70.

(54) Regeling, H.; Zwanenburg, B.; Chittenden, G. J. F.; Rehnberg, N. *Carbohydr. Res.* **1993**, *244*, 187−190.

solution of the sugar substrate (1.0 mmol) was prepared in a one-necked round-bottom flask fitted with a Schlenk stopcock. ^{t}BuMe$_2$SiH (0.3−3.3 equiv depending on the experiment performed) was added directly to a second Schlenk flask containing the catalyst PdX_2 (3 mol % with respect to sugar) in 3 mL of DMA and stirred for 1 min to give a black colloidal solution. Subsequently the sugar substrate solution was added, the apparatus connected to a gas bubbler, and the reaction stirred until hydrogen gas evolution stopped (12−24 h) and TLC indicated completion of the reaction. DMA was removed by rotary evaporation at 45 °C under full oil-pump vacuum. Flash column chromatography of the residue with ethyl acetate and hexane in various ratios removes the catalyst and yields the silylated sugars as well separated isomers. See Supporting Information for detailed spectral and other data on individual compounds.

Silylation of Sugar Substrates Using Pd(0) Black and ^{t}BuMe$_2$SiCl as the Catalyst Precursor. The procedure is identical to the one above, with the exception that Pd(0) powder is used. A suspension of Pd(0) in DMA rather than a nanocolloid is formed. Five minutes after all reagents had been combined, a catalytic amount (6 mol % with respect to palladium, i.e., 0.06 mmol) of ^{t}BuMe$_2$SiCl was added to the reaction flask. Further procedure and workup were as described above.

Silylation of Pentopyranosides Using ^{t}BuMe$_2$SiCl. (This procedure is essentially identical to the one reported by Halmos et al.[11]) A DMA or DMF (3 mL) solution of the sugar substrate (1.0 mmol) and imidazole (2.5 mmol) was prepared in a round-bottomed flask with a Schlenk stopcock. Another DMA (3 mL) solution of ^{t}BuMe$_2$SiCl (1.2 mmol) was prepared in a second Schlenk flask. The silyl chloride solution was added dropwise to the pentopyranosides and imidazole solution. After 24 h, the reactions were worked up as above.

Preparation of Samples for Dynamic Light Scattering. ^{t}BuMe$_2$SiH (1.2 mmol) was added to PdX_2 (0.03 mmol, X = Cl$^-$, OAc$^-$) suspended in dry DMA (6 mL). After 10 min, 100 μL of this solution was diluted with 4 mL of DMA to give a sample solution with an effective palladium concentration of 1.25×10^{-4} mol/L.

Preparation of Samples for TEM. ^{t}BuMe$_2$SiH (1.2 mmol) was added to PdX_2 (0.03 mmol, X = Cl$^-$, OAc$^-$) suspended in dry DMA (6 mL). After the solution was stirred for 10 min, 3 mL of sample solution was collected. The black solution was then removed from the glovebox and the specimen mounted on Formvar/carbon 200-mesh copper grids by floating the grid face down on the sample suspension for 30 s and blotting off the excess on a filter paper. To stain the samples, they were next floated on a drop of 2% w/v uranyl acetate for 10 s and then blotted.

Acknowledgment. Funding for this study was provided by the Natural Science and Engineering Research Council of Canada (NSERC), the Canadian Foundation for Innovation (CFI), the Ontario Innovation Trust Fund (OIT), Varian Canada Inc., and the University of Guelph. Electron microscopy was performed in the NSERC Guelph Regional STEM Facility, which is partially funded by an NSERC Major Facilities Access Grant.

Supporting Information Available: Comprehensive collection of 400 MHz ^{1}H and ^{13}C NMR data (COSY, HSQC) with images of spectra for all compounds and peak assignments; conditions for chromatographic isolation of the compounds and elemental analysis data for new compounds and molecular modeling coordinates for the compounds listed in Table 5 (PDF). This material is available free of charge at http://pubs.acs.org.

JA026723V